COMPUTERS AND BIOMEDICAL RESEARCH **31,** 32–46 (1998)
ARTICLE NO. CO971463

# A Computer Model of Intracranial Dynamics Integrated to a Full-Scale Patient Simulator

William James Thoman, Samsun Lampotang, Dietrich Gravenstein, and Jan van der Aa

*Department of Anesthesiology, University of Florida Brain Institute, University of Florida College of Medicine, Mowry Road, Gainesville, Florida 32608; and Department of Engineering Sciences, University of Florida College of Engineering*

Received July 31, 1997

The ability to visualize intracranial dynamics during simulated clinical scenarios is a valuable tool for teaching brain physiology and the consequences of different medical interventions on the brain. Studies have isolated physiologic variables and shown their effects on brain dynamics. However, no studies have shown the combined effects of these variables on intracranial dynamics. This brain model offers one approach that brings all these relationships together and shows how they affect the dynamics of the brain. The brain model obtains its physiologic inputs from a full-scale patient simulator which responds to clinical interventions. This integration allows individuals working on the patient simulator to see the effects of their actions on brain dynamics. The brain model gives a real-time display of intracranial events (cerebral metabolic rate, cerebral blood flow, cerebral blood volume, cerebral perfusion pressure, and intracranial pressure) and responds to changes in the pulmonary and cardiovascular condition of the patient simulator. 

## INTRODUCTION

The ability to influence intracranial dynamics is of importance to clinicians. Anesthesiologists make assumptions about intracranial pressure, neurophysiological events, and the effects of different treatments on brain dynamics. By adjusting physiologic parameters ($CMRO_2(T)$, $PaO_2$, $PaCO_2$, MABP),[1] anesthesiologists attempt to minimize and prevent brain injury.

The conceptual basis underlying the clinician's treatment strategy is derived from animal and human research literature. The present brain model provides a technique using physiological data from this same literature to generate a dynamic display of intracranial events (ICP, CBF, CBV) as they are effected by all modeled variables simultaneously. Because intracranial events are normally not evident to physicians and because this model incorporates influences of all

[1] Definitions are found in the Appendix.



0010-4809/98 $25.00

variables concurrently in real time, this brain model should be a powerful tool to teach key aspects of neurophysiology.

This model was integrated to a full-scale patient simulator (HPS v. B, Medical Education Technologies, Inc., Sarasota, FL) (*1*), which provided it real-time physiologic inputs. The simulator consists of a life-size mannequin with interactive models for the pharmacokinetics and dynamics of pharmaceuticals on the cardiopulmonary system. Real gases are used with mechanical lungs that realistically consume and produce gases. The automated breathing of the simulator is controlled by a user-adjustable arterial $CO_2$ setpoint value. The simulator can also be mechanically ventilated if desired.

The pharmacological model of the HPS appropriately and automatically alters ventilation, circulation, and neuromuscular activity in response to simulated drug administration.

The performance of the brain model was evaluated by supplying it with the physiologic data generated by a HPS that simulated trauma patients undergoing induction of general anesthesia. Repeatedly running a specific scenario on the HPS permits the influence of different management styles on intracranial dynamics to be examined.

## METHODS

ICP was modeled by assuming that the intracranial space is composed of four distinct volumes: brain (1150 mL), blood (75 mL), CSF (75 mL), and a ''mass'' (0 to 75 mL). A mass of zero represents a normal brain while a nonzero mass represents an acute abnormality (e.g., a tumor or hematoma). The normal total intracranial volume was modeled as 1300 mL (*2–4*). A total intracranial volume exceeding 1360 mL represents loss of autoregulation. Acute changes in ICP are determined by the CBV, which is related to the CBF, and the elastance (default elastance is zero in the autoregulation zone). This is based on the study by Riseberg *et al.* (*5*) that showed a linear relationship between CBV and CBF and that ICP is affected by acute changes in cerebral blood volume. Because water makes up 80% of the brain volume (*3*), the density of brain was approximated to be 1 g/mL, which allows us to use the CBF units (mL/100 g brain/min) interchangeably with the units (mL/100 mL brain/min). The relationships between the physiologic parameters ($CMRO_2$, $PaO_2$, MABP) and CBF are used to calculate CBF following the flow chart on Fig. 1. An average CBF value of 52.5 mL/100 g brain/min is used based on the literature range of 50–55 mL/100 g brain/min (*3*, *7*, *8*) and the percentage change from normal in CBF due to the physiologic parameters ($CMRO_2$, $PaO_2$, $PaCO_2$, MABP) are either added to or subtracted from 52.5 mL/100 g brain/min. The advantage of using percentage in determining the CBF is that it allows us to modify the default CBF value without having to rewrite the equations. Although we used an average CBF value, this option makes the program more flexible because individual patients can have varying CBF. All the equations are derived from graphs (Figs. 2–8) and follow the path of the flow chart in Fig. 1. Least square linear or polynomial regression fitting from Origin software (Microcal, Northampton, MA) was used

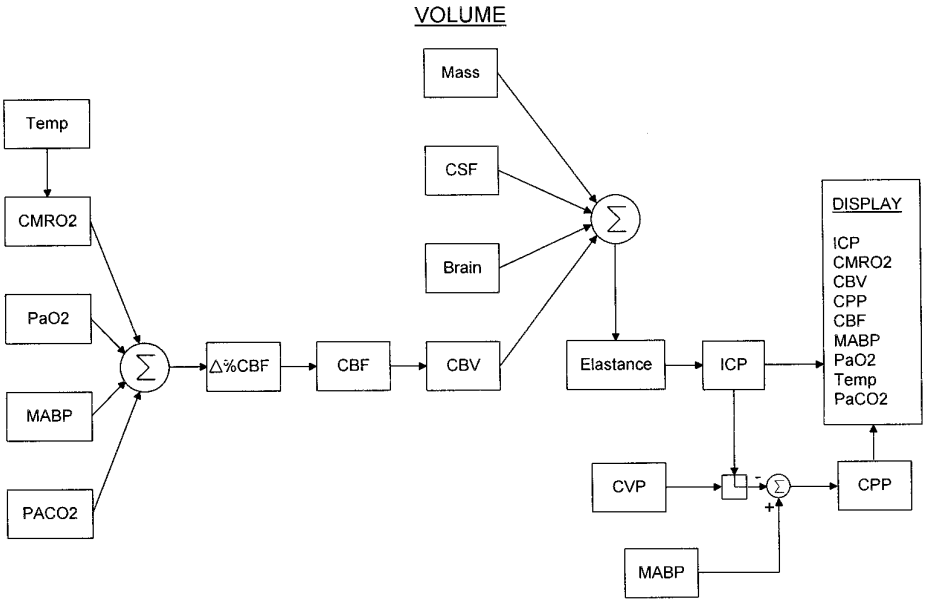


**FIG. 1.** Flow chart of ICP model.

to generate equations descriptive of these relationships. To optimize curve fit, the curves for $PaO_2$ (Fig. 2), $PaCO_2$ (Fig. 3), MABP (Fig. 6), and ICP (Fig. 8) were broken into three segments.

The HPS models temperature, $PaO_2$, $PaCO_2$, SBP, DBP, and the CVP. The brain model is interfaced with the HPS via a serial connector and updates the physiologic parameters at a sampling frequency of 10 Hertz. The brain model software uses these parameters to determine the CBF and updates both numeric and graphic displays (Figs. 9, 10, and 11) every second.

*The Effects of $PaO_2$ on CBF (Fig. 2)*

The relationship between $PaO_2$ and %CBF supported by literature (*7*) is modeled by Fig. 2. Its equations are:

1. for $0 <= PaO_2 < 40$,

$$\%CBF_{PaO_2} = 241.20908 - (2.90778 \cdot PaO_2) \quad [1]$$

2. for $40 <= PaO_2 < 61$,

$$\%CBF_{PaO_2} = 1174.3974 - 70.115107 \cdot PaO_2 + 1.7436586 \cdot (PaO_2)^2 \quad [2]$$
$$-0.01948396 \cdot (PaO_2)^3 + 8.232781\text{E} - 5 \cdot (PaO_2)^4$$

3. for $61 <= PaO_2 < 750$,

$$\%CBF_{PaO_2} = 104.47978 - 0.02543 \cdot PaO_2. \quad [3]$$

Units: $\%CBF_{PaO_2}$ (%CBF), $PaO_2$ (mmHg)

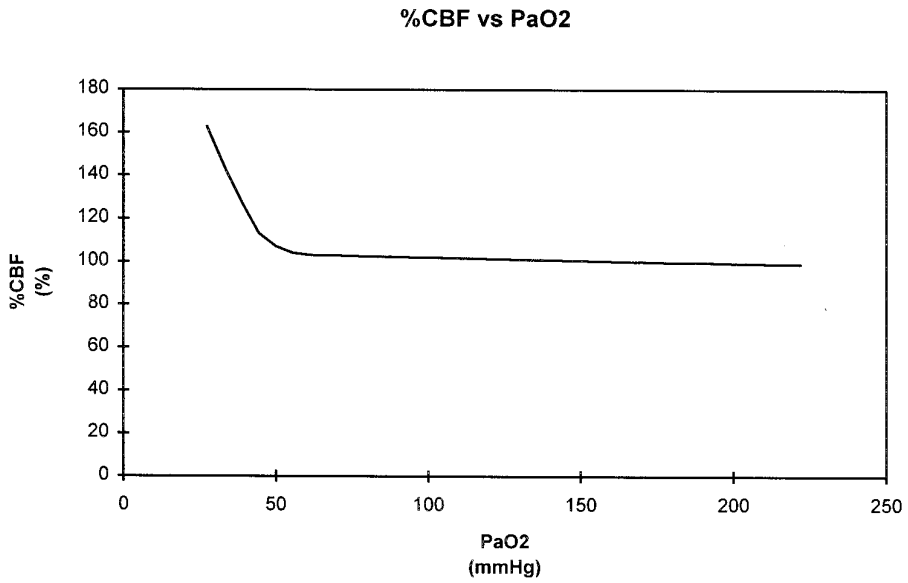


**FIG. 2.** %CBF vs $PaO_2$. The relationship between cerebral blood flow and arterial partial pressure of oxygen.

*The Effects of $PaCO_2$ on CBF (Fig. 3)*

Similar to Fig. 3, the curve *%CBF vs $PaCO_2$* that was obtained from literature (*7*) showed the curve flattening out at a $PaCO_2$ of 20 mmHg. For our purposes, the $PaCO_2$ curve was extended below a $PaCO_2$ of 20 mmHg to account for cases of hyperventilation and the lower end of the curve in Fig. 3 was redrawn in order to pass the curve through the origin. This is based on clinical concerns that during aggressive hyperventilation, CBF can be compromised sufficiently to cause ischemia. By passing the curve through the origin, we are making the effects of $PaCO_2$ more severe in that region, producing an exaggerated effect. This relationship is represented by Eqs. [4], [5], and [6] which are as follows:

1. for $0 <= PaCO_2 < 20$,

$$\%CBF_{PaCO_2} = 2.6 \cdot PaCO_2 \quad [4]$$

2. for $20 <= PaCO_2 < 80$,

$$\%CBF_{PaCO_2} = 1.76562 + 2.50347 \cdot PaCO_2 \quad [5]$$

3. for $80 <= PaCO_2 < 100$,

$$\%CBF_{PaCO_2} = 158.0634 + 0.55461 \cdot PaCO_2 \quad [6]$$

Units: $\%CBF_{PaCO_2}$ (%CBF), $PaCO_2$ (mmHg).

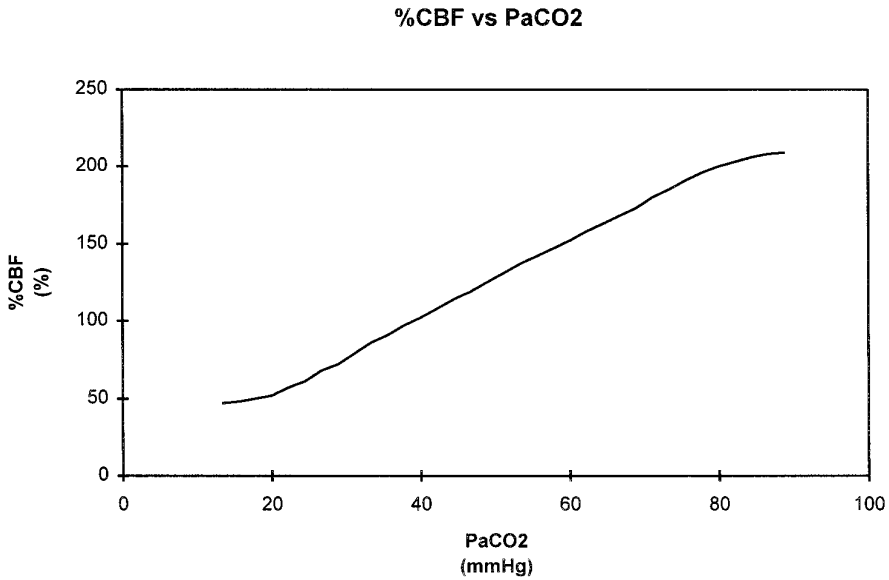


**FIG. 3.** %CBF vs $PaCO_2$. The relationship between cerebral blood flow and arterial partial pressure of carbon dioxide.

*The Effects of $CMRO_2$ on CBF (Figs. 4 and 5)*

$CMRO_2$ is not currently a HPS variable, but it is affected by temperature, which is an HPS variable. The relationship between temperature and the cerebral metabolic rate shown in Fig. 4 was obtained using Eq. [7] (*6*, *9*):

$$CMRO_2 = \exp(a + b \cdot T) \quad (a = -2.7579,\ b = 0.1089). \qquad [7]$$

The temperature and $CMRO_2$ values are displayed at the bottom of the screen (Figs. 9, 10, and 11).

As the $CMRO_2$ is updated, the percent value of the default CBF is determined continuously using Eq. [8],

$$\%CBF_{CMRO_2} = -9.88769 + 30.87319 \cdot CMRO_2 \qquad [8]$$

Units: $\%CBF_{CMRO_2}$ (%CBF), $CMRO_2$ (mL $O_2$/100 mL brain/min), T(°C).

Figure 5 shows a direct relationship between the metabolic rate and the cerebral blood flow. In contrast to the literature curve (*8*), the Y-axis of Fig. 6 was changed to %CBF with 52.5 mL/100 g brain/min representing 100%.

*The Effects of MABP on CBF (Fig. 6)*

MABP is calculated from the systolic and diastolic blood pressures using the sum of one-third SBP and two-thirds DBP. The calculated MABP is displayed at the bottom of the display monitor. Using the relationship shown in Fig. 6, the

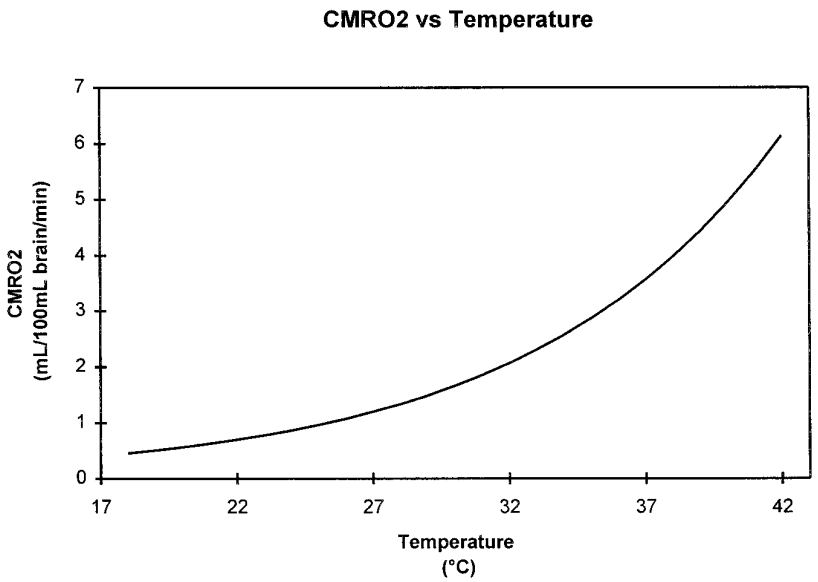


**FIG. 4.** $CMRO_2$ vs Temperature. The relationship between cerebral metabolic rate of oxygen consumption and temperature.

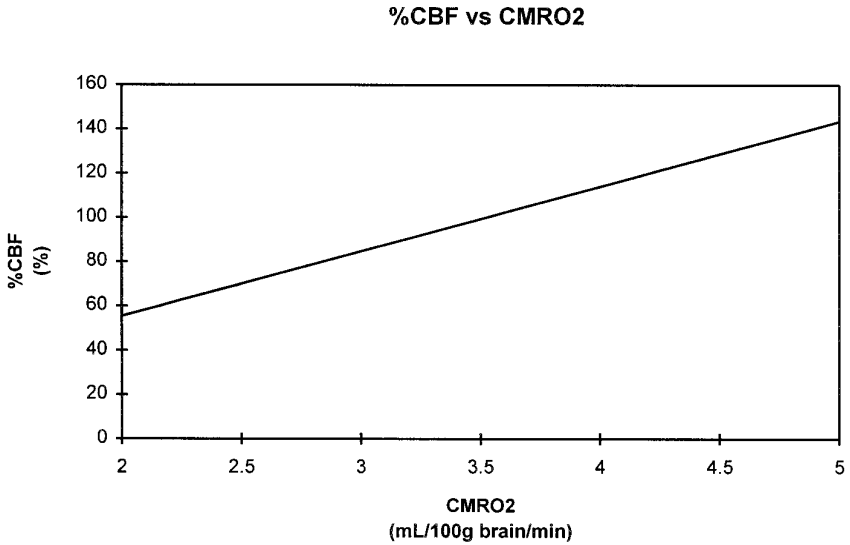


**FIG. 5.** CBF vs $CMRO_2$. The linear relationship between cerebral blood flow and the cerebral metabolic rate of oxygen consumption.

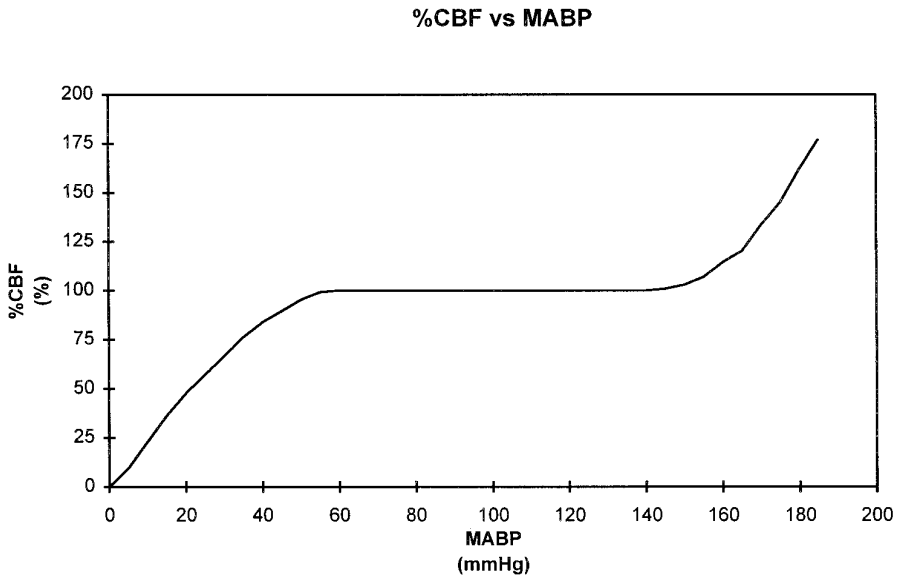


**FIG. 6.** CBF vs MABP. The relationship between cerebral blood flow and mean arterial blood pressure.

percent value of the default CBF is determined based on the MABP. In contrast to the curve shown in the literature (*3*), the Y-axis of Fig. 6 was changed to %CBF with 52.5 mL/100 g brain/min represented by 100% cerebral blood flow. Equations [9], [10], and [11] represent this relationship and are:

1. for 0 <= MABP < 60,

$$\%CBF_{MABP} = -9.3627273 + 3.8025758 \cdot MABP - 6.6594872\text{E} - 2 \cdot (MABP)^2 + 1.0904429\text{E} - 3 \cdot (MABP)^3 + 8.839161\text{E} - 6 \cdot (MABP)^4 \quad [9]$$

2. for 60 <= MABP <= 140,

$$\%CBF_{MABP} = 100 \quad [10]$$

3. for 140 < MABP < 185

$$\%CBF_{MABP} = -9824.923 + 255.15379 \cdot MABP - 2.43203203 \cdot (MABP)^2 + 1.0147878\text{E} - 2 \cdot (MABP)^3 - 1.555245\text{E} - 5 \cdot (MABP)^4 \quad [11]$$

Units: $\%CBF_{MABP}$ (%CBF), MABP (mmHg).

*Cerebral Blood Flow (CBF)*

The CBF is calculated by adding or subtracting the changes in CBF caused by $PaO_2$, $PaCO_2$, $CMRO_2(T)$, and MABP to the normal value of 52.5 mL/100 g brain/min for CBF. The %CBF from Eqs. [1]–[6], [8]–[10] are used to calculate

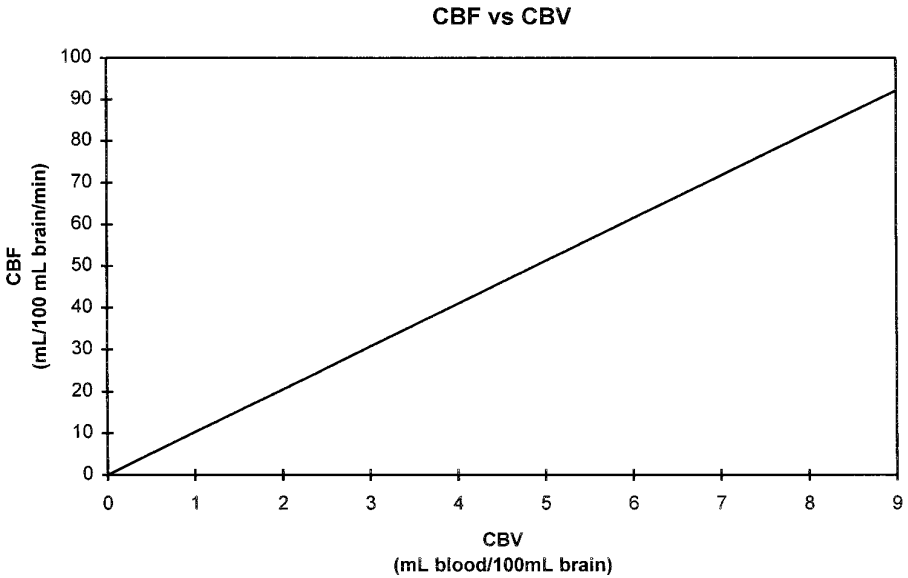


**FIG. 7.** CBF vs CBV. The linear relationship between cerebral blood flow and cerebral blood volume.

the new CBF value. Following Eq. [12], the %CBF is subtracted by 100% in order to find the percentage change in CBF. Depending on whether the change in %CBF is positive or negative the CBF will either increase or decrease. Both the numerical and grapical display of the CBF value are seen in the middle of the display monitor (Figs. 9, 10, and 11). The CBF is represented in the equation

$$\begin{aligned} CBF = 52.5 &+ (52.5 \cdot [\%CBF_{PaO_2} - 100\%] \div 100\%) \\ &+ (52.5 \cdot [\%CBF_{PaCO_2} - 100\%] \div 100\%) \\ &+ (52.5 \cdot [\%CBF_{CMRO_2} - 100\%] \div 100\%) \\ &+ (52.5 \cdot [\%CBF_{MABP} - 100\%] \div 100\%). \end{aligned} \quad [12]$$

Units: CBF (mL/100 g brain/min), $\%CBF_{CMRO_2}$ (%CBF), $\%CBF_{MABP}$ (%CBF), $\%CBF_{PaO_2}$ (%CBF), $\%CBF_{PaCO_2}$ (%CBF).

*Cerebral Blood Volume (CBV) (Fig. 7)*

From the CBF value, the CBV is determined. Figure 7 shows the linear relationship between the CBF and CBV from which the equation was obtained. The curve was fitted so that it would go through the origin by using Microsoft Excel's (Microsoft, Richmond, WA) least square regression and defining the origin as the intercept. Originally, the literature (*8*) showed a curve with a negative CBV intercept, which does not make any physiological sense. The curve shown in Fig.

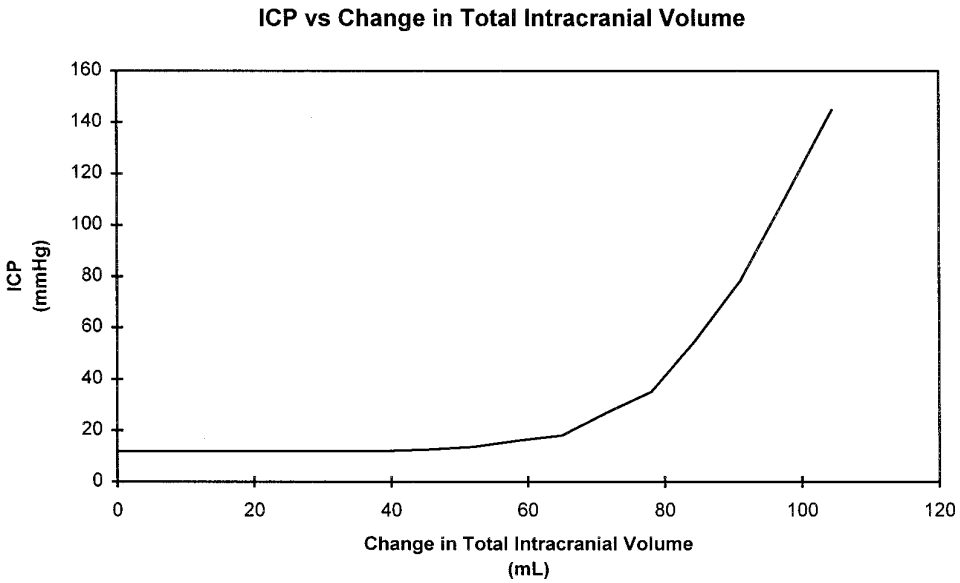


**FIG. 8.** ICP vs change in total intracranial volume. The elastance curve for intracranial pressure.

7 gave a first-order linear equation that was then rearranged to solve for CBV. The equation relating CBF to CBV is

$$CBV = \frac{15 \cdot CBF}{10.23476}. \quad [13]$$

Units: CBV (mL/100 mg brain/min), CBF (mL/100 mL brain/min).

*Intracranial Pressure (ICP) (Fig. 8)*

The elastance curve *ICP vs. Change in Total Intracranial Volume* (Fig. 8) was adapted from data on rhesus monkeys, which showed the ICP versus the volume of an intracranial balloon filled with water (*10*). In order to use the data, the ratio of human intracranial space to that of the rhesus monkey (*11*) was determined. This ratio was then used to approximately determine the change in total intracranial volume (X-axis) on Fig. 8. The total change in intracranial volume can represent changes in CBV, CSF volume, brain volume, and mass volume. The mass volume can represent an acute change in intracranial volume such as an hematoma or a gradual change such as a tumor. By entering a mass volume at the beginning of the simulation, the compensation zone of the elastance curve (flat portion) can be diminished and the ICP will respond to smaller changes in volume.

With a CBV of 75 mL there is zero change in total intracranial volume which is represented by the lower extreme left point on the elastance curve. This starting

point can be moved to the right by adding a mass volume. As the CBV increases above 75 mL we move towards the right on the elastance curve. As the CBV changes, the new ICP value is calculated based on the elastance curve. In the autoregulation area of the curve, the default value for ICP is 12 mmHg (*2*, *3*). The ICP slowly starts to increase above a 39 mL change in total intracranial volume and rapidly increases after a 60 mL change in total intracranial volume.

The ICP value is shown in the bottom curve of the display monitor (Figs. 9, 10 and 11). Using the total change in intracranial space volume with Eqs. [14], [15], and [16], the ICP value is calculated. The equations are as follows:

1. for CBV <= 39,

$$ICP = 12 \quad [14]$$

2. for 39 < CBV <= 104,

$$ICP = -21895944 + 14.990125 \cdot CBV - 0.34429666 \cdot (CBV)^2 + 3.2218647\text{E} - 2 \cdot (CBV)^3 - 9.380431\text{E} - 6 \cdot (CBV)^4 \quad [15]$$

3. for CBV > 104,

$$ICP = -479 + 6.0 \cdot CBV. \quad [16]$$

Units: ICP (mmHg), CBV (mL)

*Cerebral Perfusion Pressure (CPP)*

Using the ICP value or the CVP, the CPP is calculated using Eq. [17] or [18]. The ICP value is calculated by the brain model, while the CVP is obtained from the HPS. The CPP is determined by subtracting CVP or ICP (the larger of the two) from the MABP. The CVP or ICP represent the back pressure on the system. Maintaining an adequate CPP is important to clinicians and, in a clinical setting, it is common practice to use CVP when ICP is not monitored. Another reason for using CVP can be justified during a craniotomy since the ICP will drop to atmosphere once the dura mater is opened. The CPP is displayed on the bottom right corner of the screen (Figs. 9, 10, and 11). The equations representing CPP are as follows:

1. for CVP >= ICP,

$$\text{CPP} = \text{MABP} - \text{CVP} \quad [17]$$

2. for ICP > CVP,

$$\text{CPP} = \text{MABP} - \text{ICP} \quad [18]$$

Units: CPP (mmHg), MABP (mmHg), CVP (mmHg), ICP (mmHg).

## RESULTS

The value of the brain model is to show how intracranial dynamics are affected by patient care. To demonstrate the effects of patient management on intracranial dynamics, we ran three scenarios on the HPS that depicted a trauma case. Figures

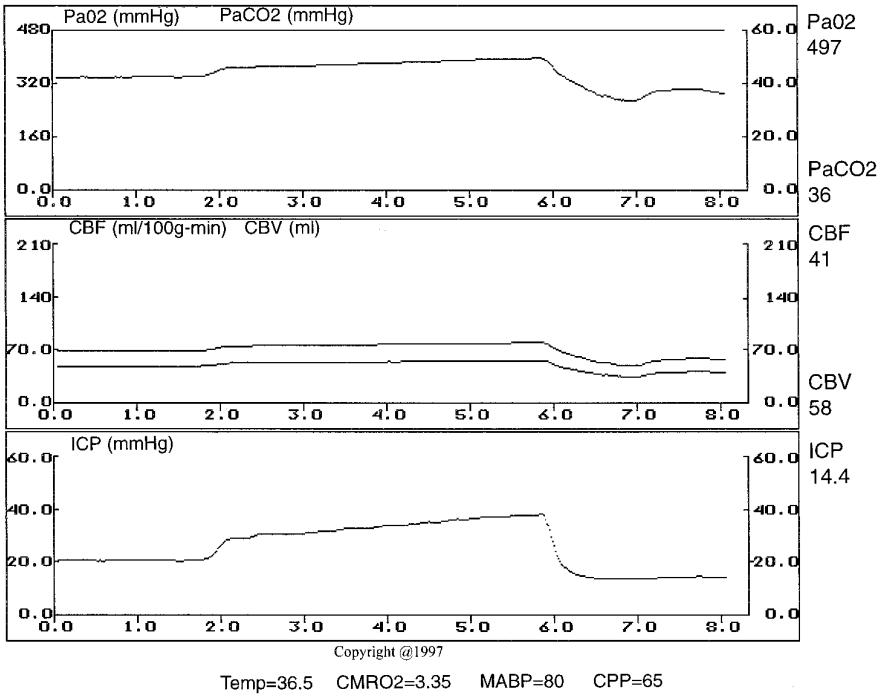


**FIG. 9.** Display of ICP model for trauma patient in scenario 1.

9, 10, and 11 show the results of the three scenarios. To show how patient care affects intracranial dynamics, we ran the same patient for all scenarios. In all cases we started with a patient who had suffered trauma, which resulted in an elevated ICP that was set at 20 millimeters of mercury. The clinicians were not informed of the elevated ICP. The brain model allows the user to enter a volume mass or the desired ICP at the beginning of each simulation. If an ICP value is entered, the brain model will calculate the approximate mass volume needed to elevate ICP according to the elastance curve (Fig. 8). This new ICP value might vary by 1 or 2 mmHg from the users value because it will have been affected by the physiological parameters. All patients were pre-oxygenated prior to arriving in the operating room. This can be seen at the top of Figs. 9, 10, and 11, where the $PaO_2$ curve is plotted.

For the first scenario, Fig. 9, an unconscious spontaneously breathing and preoxygenated patient with an elevated ICP of 22 mmHg (bottom display) comes into the operating room. One and a half minutes into the procedure (X-axis), the anesthesiologist administers 400 mg of thiopental for anesthesia and 10 mg of vecuronium for muscle relaxation. After administration of the drugs, the patient's blood pressure starts to drop and the patient becomes apneic at approximately 2 min. The $PaCO_2$ curve (top display) reveals a sharp small increment.

The ICP (lower display) increases sharply as a response to the change in carbon dioxide. This response demonstrates the linear relationship between CBF and $PaCO_2$ (Fig. 3). As the CBF increases (middle display) so does the CBV (middle display), which then results in a change in total intracranial volume causing the ICP to increase. Since the patient started with an elevated ICP, small changes in blood volume can cause significant increases in ICP. This is explained by the fact that the patient's change in total intracranial volume is located at the shoulder of the elastance curve (Fig. 8), which shows an exponential relationship. Looking at the $PaCO_2$, CBF, CBV, and ICP curves we can see that they all increase together.

Four minutes into the procedure, the anesthesiologist attempts to ventilate the patient but cannot. The anesthesiologist administers 80 mg of esmolol to reduce the effects of the laryngoscopy, which causes increases in blood pressure and heart rate. As seen in Fig. 9, the $PaCO_2$ continues to increase, which results in increases of the CBF, CBV, and ICP. Approximately, 6 min into the procedure, the clinician successfully intubates the patient and starts hyperventilating the patient. Hyperventilation causes the $PaCO_2$ to drop sharply inducing a decrease in CBF and CBV. The decrease in CBV is then reflected on the ICP, which also shows a sharp decrease. Once the patient's breathing is under mechanical ventilator control, the ICP can be managed by adjusting physiological parameters of the patient.

The second scenario (Fig. 10) shows proper clinical management of the same patient. The patient is given 400 mg of thiopental for anesthesia and 10 mg of vecuronium for muscle relaxation $1\frac{1}{2}$ min into the simulation. For this scenario the clinician suspected a possible elevated ICP and started to hyperventilate the patient after the induction of the anesthesia. There is a drop in $PaCO_2$ before the 2-min marker. This drop correlates to the drop in CBF, CBV, and ICP present at this time. The clinician keeps ventilating the patient until the patient can be intubated and mechanically ventilated. Four minutes into the procedure, the clinician administers 80 mg of esmolol and proceeds to intubate. At this point in time, there is a slight increase in $PaCO_2$, CBF, CBV, and ICP that appears on the display because the clinician temporarily stops ventilating the patient to perform the laryngoscopy and intubation. Once connected to the ventilator, the patient's breathing can be regulated in order to keep the ICP low. Notice that for this scenario, the patient's ICP was not allowed to increase from its initial value.

The third scenario (Fig. 11) shows the response of ICP to changes in MABP. The brain model display was changed in order to show the MABP curve (top display). We started with a preoxygenated simulated patient who was given 400 mg for anesthesia and 10 mg for muscle relaxation $1\frac{1}{2}$ min into the simulation. In response to the anesthetic, there is a small drop in MABP. Three minutes into the procedure, the clinician proceeds to intubate the patient without administering esmolol. The patient's sympathetic response to the laryngoscopy results in an increase in MABP (top display) and heart rate. Initially, there is no ICP response to this increase because the blood pressure is still within the autoregula-

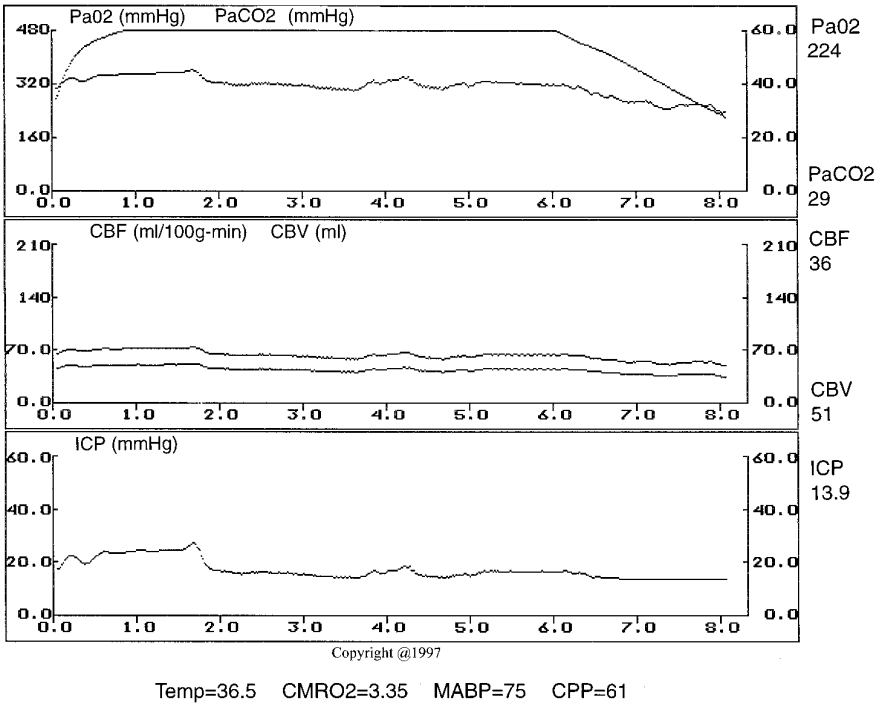


**FIG. 10.** Display of ICP model for trauma patient in scenario 2.

tion range (flat portion of Fig. 6). As blood pressure increases past the autoregulation zone limit (150 mm Hg for a normal patient), the ICP shows a sharp response to any small increments in blood pressure. The sharp response in ICP due to the MABP is demonstrated on the bottom display of Fig. 11. The effects of the laryngoscopy are short lived and the ICP rapidly returns to its original value as the MABP goes back to normal. This scenario shows the importance of maintaining hemodynamic stability in head injured victims.

## DISCUSSION AND CONCLUSION

A real time display of intracranial dynamics (Figs. 9, 10, and 11) can be a powerful tool in teaching the effects of changing physiology during patient care management. The three scenarios demonstrate how patient management is a factor in maintaining ICP. The brain model offers a straightforward approach of bringing together existing relationships between physiology and the brain found in the literature. When interfaced with a full-scale patient simulator, brain response to changes in physiology was demonstrated real time. Individuals using the simulator can see the response to their actions immediately. This is a useful tool in teaching the management of brain dynamics because most clinicians usually rely on assumptions based on the physiologic relationships used in this model.

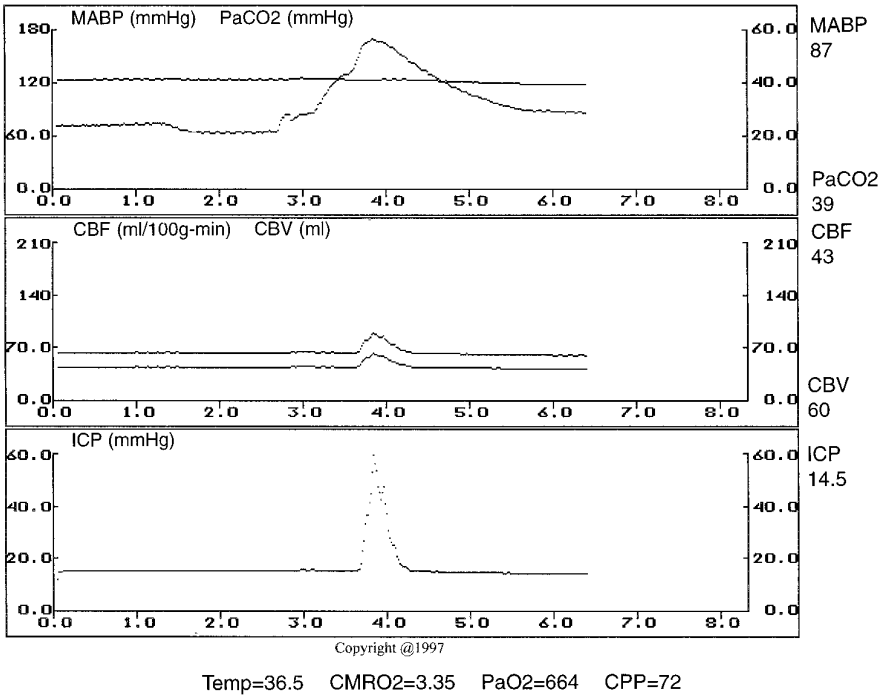


**FIG. 11.** Display of ICP model for trauma patient in scenario 3. Note the effects of MABP on intracranial pressure.

## APPENDIX: GLOSSARY

| | |
|---|---|
| CBF | Cerebral blood flow (mL/100 g brain/min) |
| CBV | Cerebral blood volume (mL/100 g brain/min) |
| $CMRO_2$ | Cerebral metabolic rate of oxygen consumption (mL/100 mL brain/min) |
| $CMRO_2(T)$ | $CMRO_2$ as a function of temperature |
| CPP | Cerebral perfusion pressure |
| CSF | Cerebrospinal fluid |
| CVP | Central venous pressure (mmHg) |
| DBP | Diastolic blood pressure (mmHg) |
| HPS | Human patient simulator |
| ICP | Intracranial pressure (mmHg) |
| MABP | Mean arterial blood pressure (mmHg) |
| $PaCO_2$ | Arterial partial pressure of carbon dioxide (mmHg) |
| $PaO_2$ | Arterial partial pressure of oxygen (mmHg) |
| SBP | Systolic blood pressure (mmHg) |
| T | Body temperature (esophageal) (°C) |
| $\%CBF_{CMRO_2}$ | Percent value of normal CBF as a function of $CMRO_2$ |

$\%CBF_{MABP}$ Percent value of normal CBF as a function of MABP
$\%CBF_{PaCO_2}$ Percent value of normal CBF as a function of $PaCO_2$
$\%CBF_{PaO_2}$ Percent value of normal CBF as a function of $PaO_2$

## ACKNOWLEDGMENTS

We thank Dr. Jan E. W. Beneken for his expertise in modeling and advice on the brain model. Also, we thank the I. Heermann Anesthesia Foundation for their support of the work on the brain model.

## REFERENCES

1. Lampotang, S., Good, M. L., van Meurs, W. L., Caravano, R. G., Azukas, J., Rueger, E. M., and Gravenstein, J. S. The University of Florida/Loral Human Patient Simulator, abstracted. *J. Anesthesia* **9,** SS1–5 (1995).
2. Lanier, W. L., Weglinski, M. R. Intracranial pressure. *In* ''Clinical Neuroanesthesia'' (R. F. Cucchiara and J. D. Michenfelder, Eds.), pp. 77–115. Churchill Livingstone, New York, 1990.
3. Sulek, C. Intracranial pressure. *In* ''Clinical Neuroanesthesia,'' 2nd ed. (S. Black, R. F. Cucchiara and J. D. Michenfelder, Eds.). Churchill Livingstone, New York, 1997.
4. Williams, W. R., ''Gray's Anatomy 35th British Ed.'' Sanders, Philadelphia, PA, 1973.
5. Riseberg, J., Ancri, D., and Ingvar, D. H. Correlation between cerebral blood volume and cerebral blood flow in the cat, *Experiments Brain Res.* **8,** 321–326 (1969).
6. Croughwell, N., Smith, L. R., Quill, T., Newman, M., Greeley, W., Kern, F., Lu, J., Reves, J. G. The effect of temperature on cerebral metabolism and blood flow in adults during cardiopulmonary bypass. *J. Thoracic Cardiovascular Surgery* **103,** 549–554 (1992).
7. Cucchiara, R. F. Cerebral blood flow and metabolism. *In* ''Clinical Neuroanesthesia'' (R. F. Cucchiara and J. D. Michenfelder, Eds.), pp. 1–40. Churchill Livingstone, New York, 1990.
8. Leenders, L., Perani, D., Lammertsma, A. A., Heather, J. D., Buckingham, P., Healy, M. J. R., Gibbs, J. M., Wise, R. J. S., Hatazawa, J., Herold, S., Beaney, R. P., Brooks, D. J., Spinks, T., Rhodes, C., Frackowiak, R. S. J., and Jones, T. Cerebral blood flow, blood volume and oxygen consumption. *Brain* **113,** 27–47 (1990).
9. Greeley, W. J., Kern, F. H., Ungerleider, R. M., *et al.* The effect of hypothermic cardiopulmonary bypass and total circulatory arrest on cerebral metabolism in neonates, infants, and children. *J. Thoracic Cardiovascular Surgery* **101,** 783–794 (1991).
10. Langfitt, T. W., Weinstein, J. D., and Kassel, N. F. Cerebral vasomotor paralysis produced by intracranial hypertension. *Neurology* **15,** 622–641 (1965).
11. Hill, W. C. O., ''Primates: Comparative Anatomy and Taxonomy,'' Halsted, New York, 1974.